Journal of Applied Polymer Science

Linear segmented polyurethanes. I. A kinetics study

Mara L. Polo [1], Marisa E. Spontón,[1] Franklin Jaramillo,[2] Diana A. Estenoz,[1] Gregorio R. Meira [1]
[1]INTEC, Universidad Nacional del Litoral—CONICET, Santa Fe, Argentina
[2]CIDEMAT, Universidad de Antioquia, Medellín, Colombia
Correspondence to: G. R. Meira (E-mail: gmeira@santafe-conicet.gov.ar)

ABSTRACT: This work investigates the two-step polymerization between methylene diphenyl diisocyanate (MDI), two different poly(tetramethylene oxide) macrodiols, and 1,4-butanediol (BD) as chain extender. At the end of the prepolymerization, the reaction mixture contains MDI in excess and a prepolymer with isocyanate end group. Then, BD and a solvent (tetrahydrofuran) were added to start the finishing stage under nominal stoichiometric equilibrium. The reaction was analyzed by Fourier transform infrared spectroscopy, hydrogen nuclear magnetic resonance (^{1}H-NMR), and size exclusion chromatography. ^{1}H-NMR was employed to follow global concentrations of unreacted isocyanate end groups and internal urethane groups. This information enabled to estimate the following "effective" rate constants: $k_1 = 1.07 \times 10^{-3}$ L mol^{-1} s^{-1} for the prepolymerization; and $k_2 = 1.94 \times 10^{-4}$ L mol^{-1} s^{-1} for the finishing stage. These values are subject to errors caused by biases introduced in the recipe, in the measurements, in the reaction conditions, in the quality of reagents, and in the reaction mechanism assumptions. Such errors also explain the dispersion of the published rate constants values. The ^{1}H-NMR measurements also enabled to estimate the evolution (with extent of reaction) of the number-average number of structural units along the prepolymerization and finishing stages; and such estimates reasonably verify Flory's classical expressions. © 2017 Wiley Periodicals, Inc. J. Appl. Polym. Sci. **2017**, *134*, 45747.

KEYWORDS: NMR; polyurethanes; reaction kinetics; SEC

Received 17 May 2017; accepted 4 September 2017
DOI: 10.1002/app.45747

INTRODUCTION

Polyurethanes (PUs) are commonly obtained by reaction between isocyanates and alcohols of functionality two or higher, in the possible presence of catalysts, solvents, and/or additives. Their properties and applications vary widely, yielding elastomers, flexible or rigid foams, fibers, sealants, adhesives, and coatings.[1,2]

The synthesis, characterization, and structure–property of linear segmented thermoplastic polyurethanes (STPUs) are active field for both academic and industrial researchers.[3] STPUs are typically prepared in two-stage polymerizations.[4,5] In the first (prepolymerization) stage, a low molar mass prepolymer is obtained by reaction between a macrodiol and an excess of diisocyanate. In the second (finishing) stage, a chain extender is added to increase the chain length. The final materials are multiblock copolymers containing "soft" segments from residues of the macrodiol, and "hard" segments from residues of the chain extender.[4] Typical (aromatic) diisocyanates are 4,4′-methylene diphenyl diisocyanate (MDI) and tolylene diisocyanate (TDI).[6] The macrodiols are generally soft aliphatic polyethers such as poly(tetramethylene oxide) (PTMO) and poly(propylene glycol) (PPG); but aliphatic polyesters and polycarbonates are also employed.[7] Typical chain extenders are low molar mass diamines or diols such as 1,4-butanediol (BD).[1] The commercial availability and relatively low toxicity of STPUs obtained from MDI and TDI has promoted an extensive research on their structure–property relationships.[8] The elastomeric characteristics of these thermoplastic elastomers are determined by their molecular structures and morphologies, with the morphologies consisting of hard microphases dispersed in soft rubber matrixes.[9] The potential application of STPUs continues to be very promising in many emerging fields such as biomaterials and tissue engineering, optoelectronics, shape-memory materials, conducting polymers, molecular recognition, smart surfaces, and others.[3]

Spaans *et al.*[10,11] controlled molecular structure in the reaction between ε-caprolactone, 1,4-butane diisocyanate (BDI), and BD. First, a new chain extender was obtained by reaction between BDI and BD in excess, and the BD in excess was removed. Second, a macrodiisocyanate was obtained by reaction between a ε-caprolactone prepolymer and BDI in excess, and the BDI in

Additional Supporting Information may be found in the online version of this article.

excess was removed. Finally, the new chain extender and the macrodiisocyanate were made to react together to produce a STPU of uniform size and longer hard segments with respect to analogous polymers synthesized via the classical two-stage procedure. Similarly, Król and Pilch-Pitera[1,12] synthesized multiblock oligomeric STPUs with narrow molar mass distributions (MMDs) and controlled chemical composition, through a sequential and non-stoichiometric multi-stage polymerization between 2,4-TDI, 2,6-TDI, and macrodiols of different molar masses and natures (polyethers and polyesters). In each stage, either a hard or a soft block was generated by bulk reaction between the oligomer synthesized in the previous stage and an excess of either TDI or the macrodiol, with extraction of the reagent in excess at each stage end. The process yielded a growing linear oligomer with either —NCO or —OH end groups, and low molar mass dispersities ($\bar{M}_w/\bar{M}_n$ between 1.1 and 1.3). Then, these oligomers could be further processed to produce either narrow-distributed STPUs or crosslinked foamed plastics or elastomers.

The synthesis of STPUs has been investigated along many decades.[1] However, many aspects of these processes are not totally elucidated. Some of the difficulties are caused by: (a) possible reaction heterogeneities; (b) high requirements for attaining stoichiometric ratios, especially when macrodiols are employed; (c) different end groups reactivities; and (d) presence of secondary reactions when, for example, solvents are included.

In the reaction between MDI, BD, and a polypropylene–polyethylene macrodiol, Castro *et al.*[13] observed early phase separation by light transmission and viscosity measurements, suggesting that a significant part of the reaction occurs in a heterogeneous medium. Later, Chen *et al.*[14] reported on the effects of reagent incompatibilities on the final STPU morphologies. Similarly, Yilgor *et al.*[5] predicted microphase separation in the synthesis of STPUs from the analysis of the solubility parameters of the reagents.

Reactivities of diols and diisocyanates depend on their molecular structure and symmetry, and on the eventual presence of substitution effects. For asymmetric diisocyanates, Speckhard *et al.*[15] theoretically suggested that narrower sequence length distributions of hard segments are produced when increasing the ratios of rate constants between primary and secondary end groups. For reactions between 2,4-TDI and 1-butanol, Caraculacu and Coseri[16] proposed a mechanism that involved four different rate constants. Similarly, Grepinet *et al.*[17,18] estimated six different rate constants for reactions between 2,4-TDI and isomers with either 2-hydroxyethyl acrylate or PPG; and Hailu *et al.*[19] determined four different rate constants for the reaction between isophorone diisocyanate (IPDI) and hydroxyl-terminated polybutadiene (HTPB). Sun and Sung[20] and Eceiza *et al.*[2] investigated the reactions without catalyst between MDI and 1-butanol (or 1-hexanol) carried out at several temperatures in cyclohexane and in the bulk, and reported identical reactivities for both isocyanate groups of MDI.

The reaction rate between alcohols and isocyanates is strongly affected by the presence of solvents. Thus, amide solvents such as dimethylformamide and *N*,*N*-dimethylacetamide (DMAc) enhance reaction rate[21]; possibly by catalyzing and increasing side reactions.[5] In contrast, aprotic solvents such as tetrahydrofuran (THF) generate alcohol–solvent complexes with strong hydrogen bonds that reduce availability of —OH groups, and decrease polymerization rate with respect to the bulk process.[21,22]

The following techniques have been employed for analyzing the synthesis of STPUs: backtitration,[18,23] hydrogen nuclear magnetic resonance (^{1}H-NMR),[24–26] carbon nuclear magnetic resonance,[27] Fourier transform infrared spectroscopy (FTIR),[20] fluorescence,[20] and size exclusion chromatography (SEC).[2,4,22,28,29] Chokki *et al.*,[24] Ckokki,[25] and Yeager and Becker,[26] analyzed composition and number-average molar mass by ^{1}H-NMR. Thompson *et al.*[28] employed SEC for determining the number-average degree of polymerization of oligomers obtained from TDI and PPG; and Lee *et al.*[4] combined a universal calibration with triple-detection SEC to determine MMD, the composition function, and the copolymer viscosity of STPUs obtained from MDI, PTMO diol, and BD. Finally, Aust and Gobec[29] employed dual-detection SEC to determine the MMD and content of hard and soft segments of prepolymers synthesized from 2,4-TDI and PTMO.[29]

A wide variety of kinetic constants has been reported for reactions between isocyanates and alcohols[2,17,18,20,22,23,27,30,31]; and Supporting Information Table S1 summarizes some of the reported values and reaction conditions. Such variety is a consequence of the combined effects of measurement errors, the large number of reagents and reaction conditions, and differences in the adopted reaction mechanisms. The investigated reactions involved either: (a) the synthesis of polymers in stoichiometric reactions between diisocyanates and low molar mass diols or macrodiols [2,20,23,27,30]; or (b) the synthesis of oligomers by reaction between macrodiols and diisocyanates in excess.[18,22] Król and Wojturska[30] reported second-order rate constants for reactions carried out in different solvents between: (i) phenyl isocyanate and low molar mass diols; and (ii) TDI and various monofunctional alcohols. For reactions between PPG and TDI Grepinet *et al.*[18] and Majoros *et al.*[22] adopted second-order kinetics. For reactions between PPG and MDI or TDI, Sun and Sung,[20] and Kothandaraman and Nasar[23] also adopted second-order kinetics, and estimated two different kinetic constant values along the extent of reaction. For reactions between 2,4-TDI and HTPB, Dubois *et al.*[27] proposed second-order kinetics, to take into account the different reactivities of isocyanate groups in *para* and *ortho* position. For MDI, Eceiza *et al.*[2] proposed a third-order rate equation based on Sato's expression,[32] that includes the catalytical effects of alcohol and urethane groups. For stoichiometric reactions between MDI and PPG, Sun and Sung[20] reported differences of up to two orders of magnitude in the rate constants when carried out in the bulk (lower values), or in DMAc (higher values). In contrast, for reactions between TDI and PPG carried out in THF, Majoros *et al.*[22] reported lower rate constant values than those reported by Kothandaraman and Nasar[23] for the same reaction, but carried out in bulk.

This work investigates the two-step synthesis represented in Scheme 1. In the prepolymerization, a PTMO diol reacts with

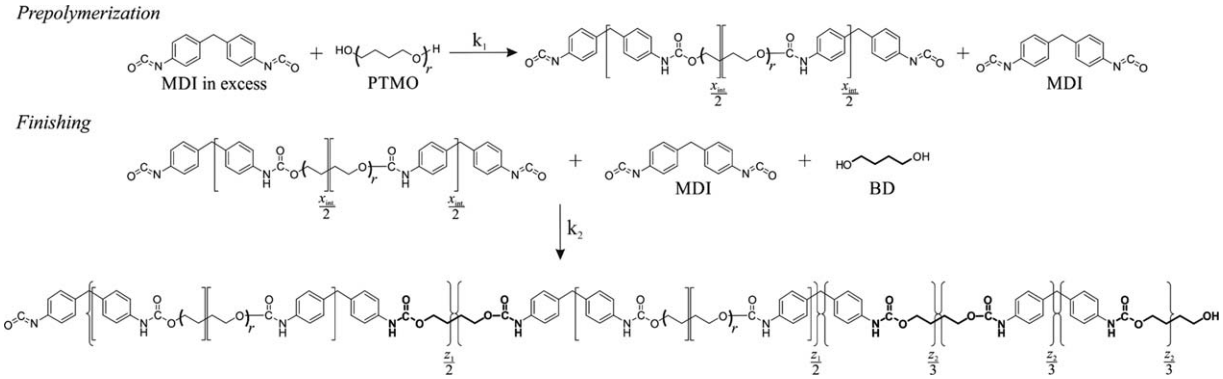

Scheme 1. Polymerization mechanism. The following nomenclature is employed in order to adapt the concept of structural units proposed by Flory.[33,34] Shown in parentheses are the r repeating units of PTMO. Along the prepolymerization, the internal structural units of the prepolymer are shown in normal square brackets, and the total number of structural units per molecule is $x = x_{int.} + 1$. The prepolymerization reagents (MDI and PTMO) contain a single structural unit. Along the finishing stage, the internal structural units are shown in curly brackets, and the total number of structural units per polymer molecule generated in the finishing stage is $z = z_1 + z_2 + 1$, where z_1 is the total number of "soft" structural units, and z_2 is the total number of "hard" structural units. The finishing reagents (prepolymer, MDI, and BD) contain a single finishing structural unit. Note the following: (1) in the prepolymerization, each structural unit contains one half of a PTMO chain length and a single urethane group; and (2) the z structural units generated in the finishing stage contain a single new urethane group. These are shown in bold font to distinguish them from the urethane groups generated in the prepolymerization (in normal font).

an excess of MDI to produce a low molar mass prepolymer containing only isocyanate end groups. In the finishing stage, BD is added, the system is diluted with THF, and the —OH groups in BD react with the isocyanate groups in the polymer and unreacted MDI. The reactions were followed by FTIR, ^{1}H-NMR, and SEC. The ^{1}H-NMR measurements were employed to adjust the k_1 and k_2 kinetic constants, and to estimate the evolution (with extent of reaction) of the number-average number of structural units along prepolymerization and finishing. These evolutions were compared to theoretical predictions by classical expressions originally developed for reactions between AA and BB comonomers.[33,34] The SEC results are employed in the second part of this sequel, to verify a new comprehensive polymerization model.

POLYMERIZATIONS

The reagents (MDI, BD, and two different PTMO macrodiols) were all from Sigma Aldrich (Saint Louis, MO). Table I presents three different estimates of the number-average molar masses ($\bar{M}_n$) of the employed macrodiols. One of such estimates was provided by the manufacturer (Sigma Aldrich); while the other two were determined in this work as follows: one of them by following the same ASTM procedure as the manufacturer, and the other by SEC, as explained below.

The solvents THF and methanol were from Cicarelli (Argentina), and were dried by distillation under nitrogen prior to use. THF was distilled from sodium/benzophenone, and methanol was distilled from magnesium sulfate. The sodium (99%) was from Tetrahedron (Argentina); the benzophenone (≥99%) was from Merck (Höhenbrunn, Germany); and the magnesium sulfate was from Cicarelli (Argentina). The ^{1}H-NMR samples contained deuterated dimethyl sulfoxide (DMSO-d_6) from Sigma Aldrich, and styrene monomer from Petrobras (Argentina) that was distilled prior to use.

The reactions were carried out in three-necked 100-mL glass flasks with magnetic stirring. Reaction temperatures were controlled at 60 °C by means of a heated oil bath and a reflux condenser.

The FTIR spectrophotometer was a Perkin Elmer Spectrum One with Fourier Transform, wavelength range 400–4000 cm^{-1}, resolution 4 cm^{-1}, and ClNa cell windows. The ^{1}H-NMR spectrophotometer was a 300 MHz Brüker Avance with Fourier transform. The size exclusion chromatograph was a Waters Model 1525, fit with an automatic injector (Waters 717), two fractionation columns (Waters Styragel HR1 and HR4), and a differential refractometer (Waters 2414). The carrier solvent was THF at 1 mL min^{-1}, and the system was operated at ambient temperature.

Five experiments were carried out at 60 °C; and their recipes are detailed in Table II. Note the following: (a) the PTMO masses were estimated from the $\bar{M}_n$ values reported by the manufacturer (Table I); (b) the experiments with identical global molar ratios involved different macrodiols; and (c) Experiments 1 and 3 employed larger relative masses of MDI and BD compared to experiments 2 and 4, and were therefore expected to produce

Table I. Estimates of the Number-Average Molar Masses of the Two Employed Macrodiols

	$\bar{M}_n$ (g mol^{-1})	
Method	$PTMO_1$	$PTMO_2$
ASTM 4274-9[a]	997	2024
ASTM 4274-9[b]	1100	2100
SEC[b]	880	2180

[a] According to the manufacturer.
[b] Determined in this work.

Table II. Polymerization Experiments: Recipes and Global Measurements

		Experiment 1	Experiment 2	Experiment 3	Experiment 4	Experiment 5
Recipe						
[MDI]/[PTMO]/[BD]		1.0/0.3/0.7	1.0/0.7/0.3	1.0/0.3/0.7	1.0/0.7/0.3	1.0/0.5/0.5
Prepolymerization						
MDI	(g)	1.677	1.001	1.677	0.743	1.677
	(mol)	6.70×10^{-3}	4.00×10^{-3}	6.70×10^{-3}	2.97×10^{-3}	6.70×10^{-3}
$PTMO_1$[a]	(g)	2.004	2.792	—	—	3.341
	(mol)	2.01×10^{-3}	2.80×10^{-3}			3.35×10^{-3}
$PTMO_2$[b]	(g)	—	—	4.069	4.207	—
	(mol)			2.01×10^{-3}	2.08×10^{-3}	
Finishing						
BD	(g)	0.423	0.108	0.423	0.080	0.302
	(mol)	4.69×10^{-3}	1.20×10^{-3}	4.69×10^{-3}	0.89×10^{-3}	3.35×10^{-3}
THF	(mL)	20	20	20	20	20
Measurements at the prepolymerization end ($t_{Prep.} = 2$ h)						
n_{-NCO}	(mol)	7.52×10^{-3}[c,d]	—	—	—	—
		8.11×10^{-3}[c,e]				
$n_{-NHCOO-}$	(mol)	2.74×10^{-3}[c,f]	—	—	—	—
$\bar{M}_{n,Pol.}$	(g mol^{-1})	1700[g]	5580[g]	3040[g]	6950[g]	2830[g]
$\bar{M}_{w,Pol.}$	(g mol^{-1})	3690[g]	13,400[g]	8740[g]	16,500[g]	6680[g]
$\bar{M}_{n,Global}$	(g mol^{-1})	890[g]	5580[g]	1520[g]	6600[g]	2050[g]
		980[c,h]				
		910[c,i]				
$\omega_{MDI,Prep.}$	(—)	0.158[g]	~0[i]	0.090[i]	0.002[i]	0.037[i]
Measurements at the end of the finishing stage ($t_{Fin.} = 43$ h)						
n_{-NCO}	(mol)	~ 0[c]	—	—	—	—
$n_{-NHCOO-}$	(mol)	1.08×10^{-2}[c,f]	—	—	—	—
$\bar{M}_{n,Pol.}$	(g mol^{-1})	6840[g]	12,300[g]	11,000[g]	8150[g]	9160[g]
$\bar{M}_{w,Pol.}$	(g mol^{-1})	41,500[g]	52,600[g]	51,300[g]	52,500[g]	46,900[g]

[a] Based on $\bar{M}_{n,PTMO_1} = 997$ g mol^{-1} (manufacturer data).
[b] Based on $\bar{M}_{n,PTMO_2} = 2024$ g mol^{-1} (manufacturer data).
[c] By ^{1}H-NMR.
[d] Moles of —NCO end groups estimated from peak a and eqs. (1a) and (2).
[e] Moles of —NCO end groups estimated from peak b and eqs. (1b) and (2).
[f] Moles of —NHCOO— groups estimated from peak f and eqs. (3) and (4).
[g] By SEC.
[h] From peak a and eq. (7).
[i] From peak b and eq. (7).

higher concentrations of hard segments. The final global results are in the lower half of Table II.

Prior to the reactions, the PTMO prepolymers were dried under vacuum at 100 °C for 1 h. For the prepolymerizations, the macrodiol was mixed with MDI in excess, and the reaction was carried out at 60 °C for 2 h under inert gas (N_2). Then, anhydrous THF and BD were added, and the finishing stage was carried out at 60 °C for 43 h, until the total conversion of isocyanate groups, as verified by FTIR. Due to the low quantities of reagents employed, in each experiment, two prepolymerizations were carried out in parallel. One of such reactions was used to produce prepolymerization samples of about 0.5 mL, and then it was stopped. Then, the finishing stage was continued in the second reactor alone, and (due to the dilution with THF) larger volume samples of about 1 mL were taken. In experiment 1, the reaction volumes were $V_{Prep.} = 3.49$ mL for the prepolymerization, and $V_{Fin.} = 23.1$ mL for the finishing stage.

The samples for FTIR were directly frozen and employed as such. The samples for ^{1}H-NMR and SEC were derivatized with methanol and dried prior to use. The derivatizations were carried out at ambient temperature, and involved transformation of the unreacted —NCO end groups into methyl-terminated urethane end groups (—$NHCOOCH_3$); see molecular structures at the top and bottom of Figure 2. After derivatization, the solvents (i.e., the unreacted methanol and the THF contained in the finishing samples) were eliminated by casting under vacuum

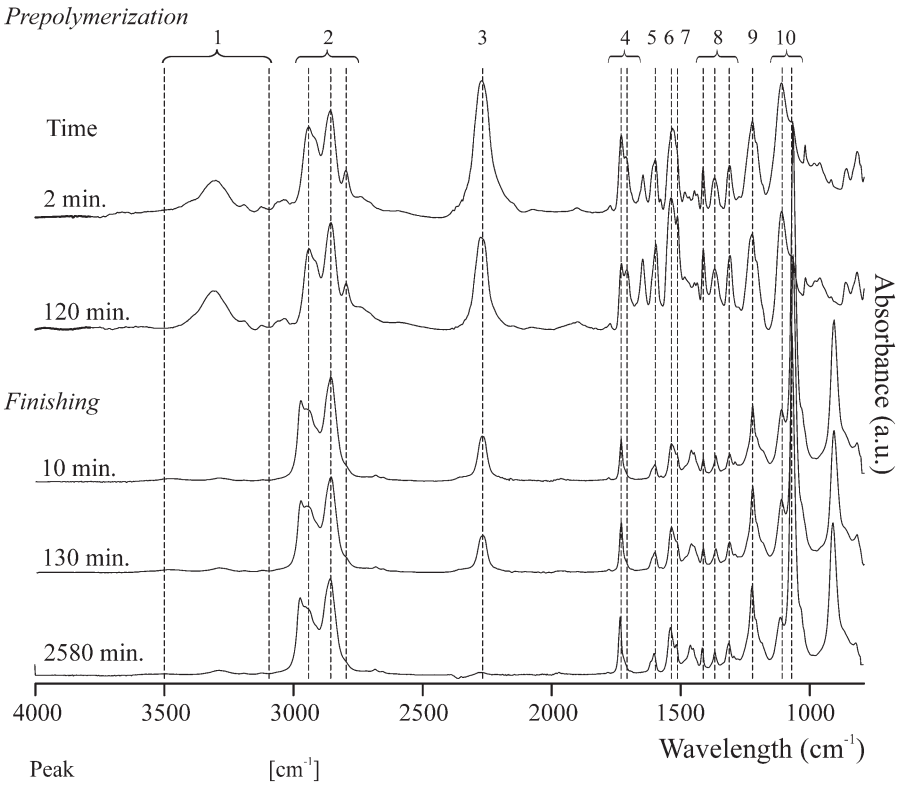

Peak		[cm^{-1}]	
1	3500-3100	–N–H, –O–H	Stretching vibrations (str. vibr.), with and without H-bonds
2	2938, 2853, 2795	–CH_2–	Methylene str. vibr. (asymm. and symm. modes)
3	2273	–N=C=O	Isocyanate str. vibr.
4	1727, 1698	–C=O	Str. vibrs of free- and hydrogen-bonded carbonyl urethanes
5	1596	–C=C–	Aromatic ring, framework vibr.
6	1529	–C–N–	Str. vibr. mode (Amide II)
7	1479	–N–H	Bending mode
8	1413, 1365, 1307	–CH_2–	Methylene bending and wagging modes
9	1218	–C–N–	Str. vibr. mode (Amide III)
10	1103, 1074	–C–O–C–	Ether and urethane str. vibr. modes

Figure 1. FTIR spectra of experiment 1, at five reaction times. Note the disappearance of —NCO groups at reaction end.

at ambient temperature. This procedure did not eliminate the unreacted MDI, but did eliminate the unreacted BD contained in the finishing samples.

RESULTS AND DISCUSSION

FTIR Measurements

For experiment 1, Figure 1 shows the FTIR spectra at five reaction times. The absorption band at 2273 cm^{-1} characterizes the isocyanate groups, and (as expected) it decreases in intensity until total disappearance at the reaction end. Also, note the reduction of peaks at 3500–3100 cm^{-1}, due to N—H hydrogen bonds and —OH stretchings.

^{1}H-NMR Measurements

For experiment 1, the ^{1}H-NMR samples were prepared by dissolving around 40 mg of the derivatized and dried reaction samples in 0.6 mL of deuterated DMSO, plus addition of around 12 mg of styrene as internal standard. Figure 2 presents the spectra at six reaction times, with identification of peaks. Note the following: (a) peaks a and b enable to independently determine the number of terminal methyl groups generated by derivatization; while (b) peak f enables to determine the number of internal urethane units. The quantification involved determination of the areas under peaks a, b, and f, and under the s duplets at 5.80–5.86 ppm of the internal standard (Figure 2). Peaks b and f were deconvoluted by the provided software, and the final measurements are presented in Supporting Information Table S2. Consider now the applied calculation procedures.

Global End Groups. Along the reaction, the total moles of terminal methyl groups in the ^{1}H-NMR samples ($n_{-CH_3|_{^1H\text{-}NMR}}$) were independently estimated from peaks a and b through

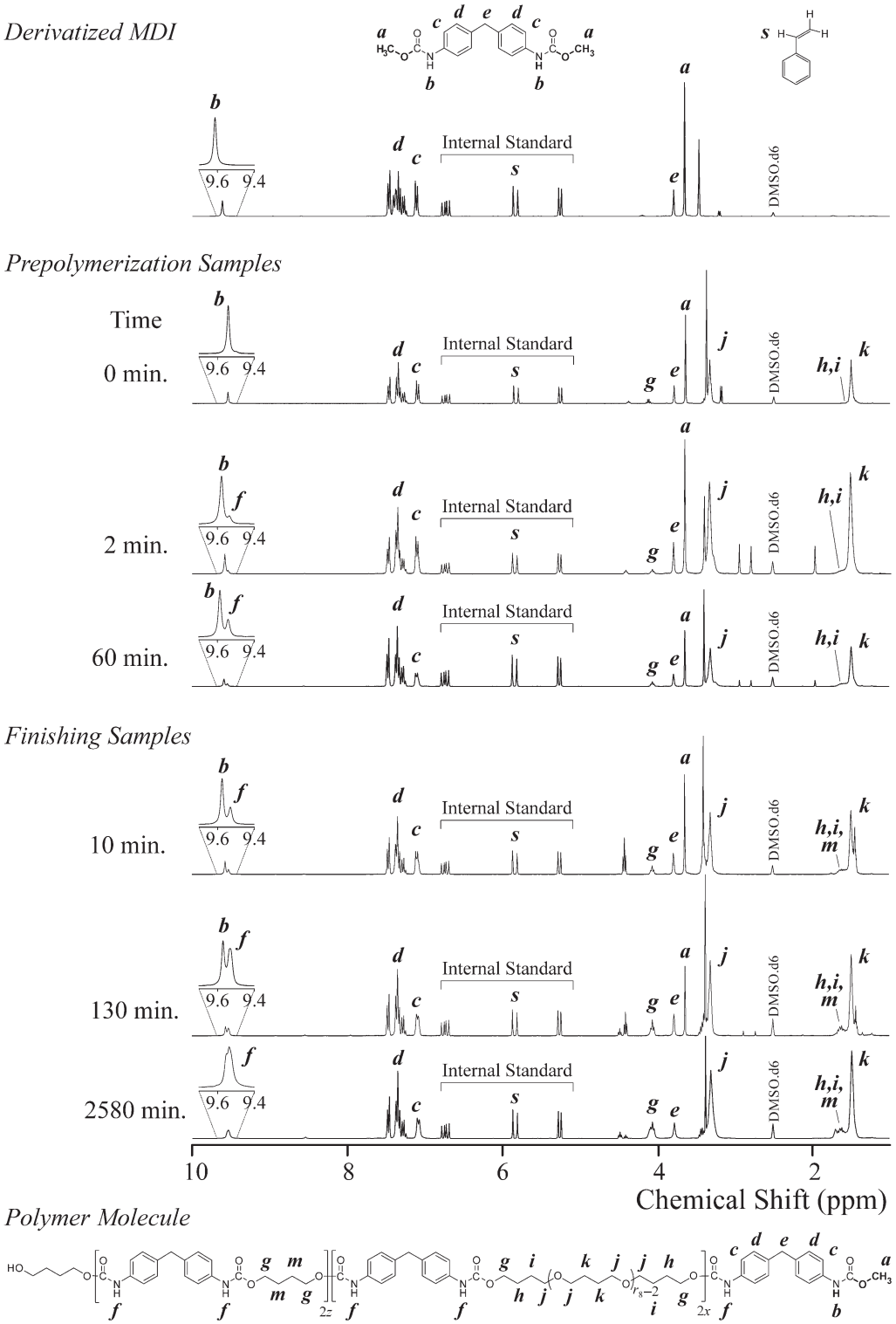

Figure 2. Experiment 1: ^{1}H-NMR spectra of the derivatized initial MDI and derivatized polymer samples at several reaction times (see the corresponding molecular structures with identified protons). The quantification involved protons contained in: (i) methyl end groups (peaks a and b); (ii) urethane internal groups (peaks f); and (iii) s duplet at 5.86 and 5.80 ppm of the internal (styrene) standard. The ^{1}H-NMR results are in Supporting Information Tables S2 and S3.

$$n_{-CH_3}|_{^1\text{H-NMR}} = n_{St}|_{^1\text{H-NMR}} \frac{(\text{Area under peak a})/3}{\text{Area under St duplet}} \quad (1a)$$

$$n_{-CH_3}|_{^1\text{H-NMR}} = n_{St}|_{^1\text{H-NMR}} \frac{\text{Area under peak b}}{\text{Area under St duplet}} \quad (1b)$$

Table III. Experiment 1: ^{1}H-NMR and SEC Results

	^{1}H-NMR Results											
	Prepolymerization											
	Through peak *f*	Through peak *a*			Through peak *b*			SEC Results			
$t_{Prep.}$ (min)	$n_{-NHCOO-,Prep.}$[a] (mol)	$n_{-NCO,Prep.}$[b] (mol)	$p_{Prep.}$[c] (—)	$\bar{x}_{n,Prep.}$[d] (—)	$n_{-NCO,Prep.}$[b] (mol)	$p_{Prep.}$[c] (—)	$\bar{x}_{n,Prep.}$[d] (—)	$\bar{M}_{n,Pol.}$ (g mol^{-1})	$\bar{M}_{w,Pol.}$ (g mol^{-1})	$\omega_{MDI,Prep.}$ (—)	$\bar{M}_{n,Global\ Prep.}$ (g mol^{-1})
0	0.00	1.11×10^{-2}	0.00	1.00	1.06×10^{-2}	0.00	1.00	880	1700	0.455	410
2	1.23×10^{-3}	1.11×10^{-2}	0.37	1.19	1.08×10^{-2}	0.39	1.19	1310	2360	0.358	520
7	2.32×10^{-3}	8.99×10^{-3}	0.70	1.46	8.50×10^{-3}	0.73	1.50	1650	3110	0.234	710
15	3.01×10^{-3}	8.09×10^{-3}	0.90	1.71	7.83×10^{-3}	0.95	1.75	1830	3480	0.194	820
30	3.14×10^{-3}	7.73×10^{-3}	0.94	1.79	7.45×10^{-3}	0.99	1.84	1690	3540	0.186	820
60	2.83×10^{-3}	7.83×10^{-3}	0.85	1.68	7.30×10^{-3}	0.89	1.74	1580	3380	0.205	760
120	2.74×10^{-3}	7.52×10^{-3}	0.82	1.67	8.11×10^{-3}	0.86	1.64	1700	3690	0.158	890
	Finishing										
	Through peak *f*	Through peak *a*			Through Peak *b*						
$t_{Fin.}$ (min)	$n_{-NHCOO-,Prep.}$a (mol)	$n_{-NCO,Fin.}$[b] (mol)	$p_{Fin.}$[e] (—)	$\bar{z}_{n,Fin.}$[f] (—)	$n_{-NCO,Fin.}$[b] (mol)	$p_{Fin.}$[e] (—)	$\bar{z}_{n,Fin.}$[f] (—)	$\bar{M}_{n,Pol.}$ (g mol^{-1})	$\bar{M}_{w,Pol.}$ (g mol^{-1})	$\omega_{MDI,Fin}$ (—)	$\bar{M}_{n,Global\ Fin.}$ (g mol^{-1})
0	2.74×10^{-3}	7.52×10^{-3}	0.82	1.67	8.11×10^{-3}	0.86	1.64	1700	3690	0.158	890
10	3.32×10^{-3}	8.13×10^{-3}	—	—	7.10×10^{-3}	0.13	1.08	1050	2820	[g]	[g]
130	4.94×10^{-3}	4.20×10^{-3}	0.44	1.53	4.00×10^{-3}	0.51	1.55	1920	4980	[g]	[g]
1120	4.33×10^{-3}	3.29×10^{-4}	0.96	5.83	1.44×10^{-4}	0.98	12.04	6870	39,100	[g]	[g]
1630	9.24×10^{-3}	6.16×10^{-5}	0.99	106	0.00	—	—	6580	39,000	[g]	[g]
2580	1.08×10^{-2}	3.60×10^{-5}	1.00	225	0.00	—	—	6840	41,500	[g]	[g]

[a] No. of moles of urethane internal groups estimated from eq. (4).
[b] No. of moles of isocyanate end groups estimated from eq. (2).
[c] Extent of reaction estimated from eqs. (5) and (8a).
[d] Number-average number of structural units estimated from eqs. (2), (4), (5), and (9a).
[e] Extent of reaction estimated from eqs. (2) and (8b).
[f] Number-average number of structural units estimated from eqs. (2), (4), (6), and (9b).
[g] Chromatograms do not provide information of unreacted MDI or BD.

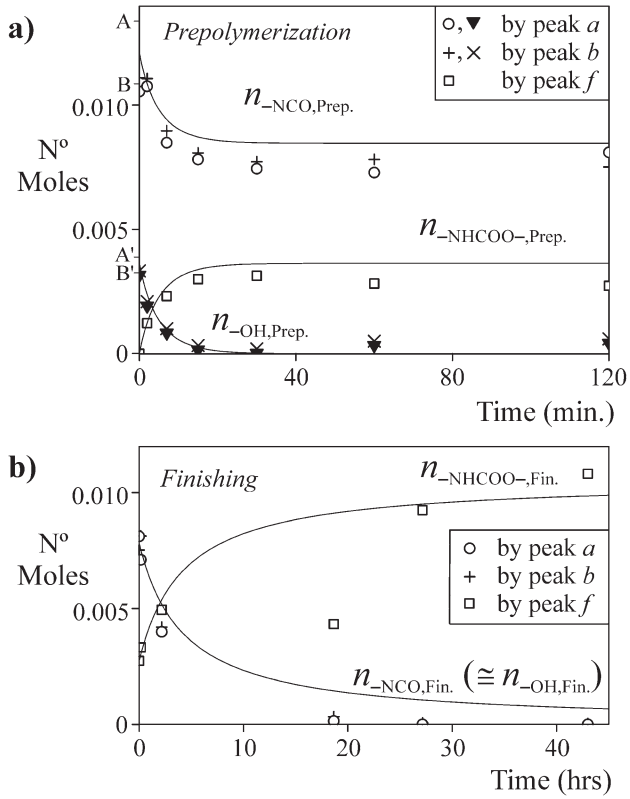

Figure 3. Experiment 1: Concentration determinations by ^{1}H-NMR along: (a) the prepolymerization; and (b) the finishing stage. The model predictions are shown in continuous trace, and were obtained through eq. (12) with $k_1' = 0.307$ mol^{-1} s^{-1} and $k_2' = 8.39 \times 10^{-3}$ mol^{-1} s^{-1}, i.e., the corresponding values of k_1 and k_2 in Table IV. To adjust the prepolymerization rate constant, two different sets of initial concentrations n^0_{-NCO} and n^0_{-OH} were adopted, that are indicated in (a) as (A,A′), and (B,B′).

where $n_{St}|_{^1H\text{-}NMR}$ (= 0.012 mg/104.15 g mol^{-1}) are the moles of the internal standard in the ^{1}H-NMR samples (Supporting Information Table S2). Then, the total moles of original —NCO end groups in the reaction mixture (n_{-NCO}) were estimated from the moles of —CH_3 groups in the ^{1}H-NMR samples ($n_{-CH_3}|_{^1H\text{-}NMR}$) through

$$n_{-NCO} = n_{-CH_3}|_{^1H\text{-}NMR} \frac{g_{\text{Reaction Mixture}}}{g_{\text{Deriv. Sample}}} \quad (2)$$

where $g_{\text{Deriv. Sample}}$ is the mass of the derivatized ^{1}H-NMR samples; and $g_{\text{Reaction Mixture}}$ is the mass of reagents and products (i.e., not including the solvent added in the finishing stage).

The number of internal urethane groups in ^{1}H-NMR samples ($n_{-NHCOO-}|_{^1H\text{-}NMR}$) was obtained from

$$n_{-NHCOO-}|_{^1H\text{-}NMR} = n_{St}|_{^1H\text{-}NMR} \frac{\text{Area under peak f}}{\text{Area under St duplet}} \quad (3)$$

and the total urethane moles in the reaction mixture ($n_{-NHCOO-}$) were obtained from

$$n_{-NHCOO-} = n_{-NHCOO-}|_{^1H\text{-}NMR} \frac{g_{\text{Reaction Mixture}}}{g_{\text{Deriv. Sample}}} \quad (4)$$

Along the prepolymerization, the number of —OH end groups $n_{-OH,Prep.}$ was estimated from:

$$n_{-OH,Prep.} = 2\ n^0_{PTMO} - n_{-NHCOO-,Prep.} \quad (5)$$

where n^0_{PTMO} is the initial moles of PTMO. The finishing stage was carried out under stoichiometric equilibrium, and the moles of unreacted —OH end groups ($n_{-OH,Fin.}$) nominally coincide with the moles of —NCO end groups, i.e.,

$$n_{-OH,Fin.} \cong n_{-NCO,Fin.} \quad (6)$$

Table III and Figure 3(a,b) present the ^{1}H-NMR estimates obtained through eqs. (1)–(6). Note that peaks a and b provide similar estimates for the reduction of —NCO end groups along the reaction, and that such reduction corresponds to an equivalent increase in internal urethane groups [Figure 3(a,b)]. Also, note that at the beginning of each stage, the ^{1}H-NMR estimates of —NCO end groups are below their nominal recipe values (Table II).

Global Number-Average Molar Mass at Prepolymerization End. At the Prepolymerization end ($t_{Prep.} = 120$ min), all the PTMO has reacted, and the molecules only contain —NCO end groups. Thus, the total reaction moles are ($n_{-NCO,Prep.}$); and $\bar{M}_n$ of the global reaction mixture is

$$\bar{M}_{n,Global}(t_{Prep.} = 120 \text{ min}) = \frac{\text{Total Prepolymerization Mass}}{\text{Total Prepolymerization Moles}} = \frac{g_{Prepol.}}{n_{-NCO,Prep.}/2} \quad (7)$$

where $g_{Prepol.}$ is the mass of reagents and products in the prepolymerization stage. Introducing the $n_{-NCO,Prep.}$ estimates from peaks a and b into eq. (7), the following global $\bar{M}_n$ values were obtained at the prepolymerization: 980 g mol^{-1} for peak a, and 910 g mol^{-1} for peak b (Table II).

Number-Average Number of Structural Units versus Extent of Reaction. Call $p_{Prep.}$ and $p_{Fin.}$ the extents of reaction along the prepolymerization and finishing stages, respectively. Such variables are based on the consumption of end groups in defect. Thus, along the prepolymerization, one has

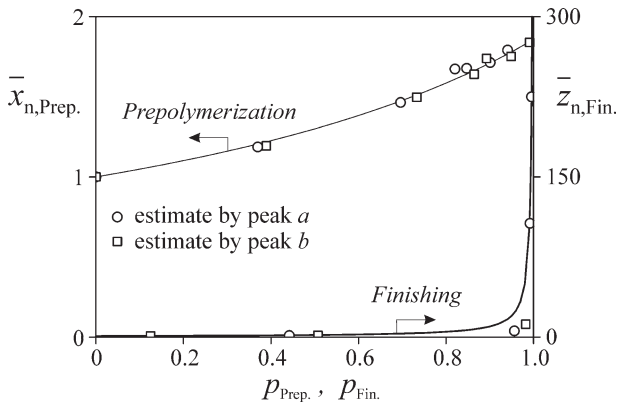

Figure 4. Evolution of the number-average number of structural units with the extent of reaction along the prepolymerization and finishing stages [$\bar{x}_{n,Prep.}(p_{Prep.})$ and $\bar{z}_{n,Fin.}(p_{Fin.})$, respectively]. The experimental points also required estimation of the extents of reaction [eqs. (8a) and (8b)]. The model predictions are in continuous trace, and were directly obtained through eq. (14a) with $r = 0.3$ for the prepolymerization, and through eq. (14b) for the finishing stage.

$$p_{\text{Prep.}} = \frac{n^0_{-\text{OH,Prep.}} - n_{-\text{OH,Prep.}}}{n^0_{-\text{OH,Prep.}}} \quad (8a)$$

where $n^0_{-\text{OH,Prep.}}$ and $n_{-\text{OH,Prep.}}$ are the initial and residual moles of —OH end groups. Along the finishing stage, the following equation was employed

$$p_{\text{Fin.}} = \frac{n^0_{-\text{NCO,Fin.}} - n_{-\text{NCO,Fin.}}}{n^0_{-\text{NCO,Fin.}}} \quad (8b)$$

where $n^0_{-\text{NCO,Fin.}}$ and $n_{-\text{NCO,Fin.}}$ are the initial and residual moles of —NCO end groups along the finishing stage. At the beginning of the finishing stage, it was assumed that the moles of —NCO groups coincide with the moles of —NCO end groups at the prepolymerization end, i.e., $\left[n_{-\text{NCO,Prep.}}\left(t_{\text{Prep.}} = 120\ \text{min}\right) = n^0_{-\text{NCO,Fin.}}\right]$.

From Scheme 1, the global number-average number of structural units generated along the prepolymerization and finishing stages ($\bar{x}_{n,\text{Prep.}}$ and $\bar{z}_{n,\text{Fin.}}$, respectively) were estimated from the ratios between the total number of structural units and the total number of moles. In any polymer molecule, the terminal units contribute with a single structural unit; and therefore, the total number of terminal structural units coincides with total number of moles $(n_{-\text{OH}}/2 + n_{-\text{NCO}}/2)$. Along the prepolymerization, the total number of internal structural units is given by $\left(n_{-\text{NHCOO}-,\text{Prep.}}\right)$, and then one can write

$$\bar{x}_{n,\text{Prep.}} = \frac{n_{-\text{NHCOO}-,\text{Prep.}} + \left(n_{-\text{OH,Prep.}}/2\right) + \left(n_{-\text{NCO,Prep.}}/2\right)}{\left(n_{-\text{OH,Prep.}}/2\right) + \left(n_{-\text{NCO,Prep.}}/2\right)} \quad (9a)$$

Along the finishing stage, only the newly-generated urethane moles generate z internal structural units (Scheme 1). Therefore, the total number of z internal structural units is given by the difference between the total number of urethane moles $(n_{-\text{NHCOO}-})$ and the moles of urethanes generated in the prepolymerization, i.e., $n_{-\text{NHCOO}-,\text{Prep.}}(t_{\text{Prep.}} = 120\ \text{min})$. Thus, one can write

$$\bar{z}_{n,\text{Fin.}} = \frac{\left(n_{-\text{NHCOO}-} - n_{-\text{NHCOO}-,\text{Prep.}}(t_{\text{Prep.}} = 120\ \text{min})\right) + \left(n_{-\text{OH,Fin.}}/2\right) + \left(n_{-\text{NCO,Fin.}}/2\right)}{\left(n_{-\text{OH,Fin.}}/2\right) + \left(n_{-\text{NCO,Fin.}}/2\right)} \quad (9b)$$

For experiment 1, eqs. (8a), (9a) and (8b), (9b) enabled to calculate the pairs $\left(p_{\text{Prep.}}, \bar{x}_{n,Prep.}\right)$ and $\left(p_{\text{Fin.}}, \bar{z}_{n,\text{Fin.}}\right)$, respectively; and the results are presented in Table III and Figure 4. Note that $\bar{x}_{n,\text{Prep.}} \cong 1.65$ at the prepolymerization end, while $\bar{z}_{n,\text{Fin.}} \cong 225$ at the end of the finishing stage.

SEC Measurements

The SEC samples were prepared by dissolving the derivatized and dry reaction samples in THF (0.4% wt/vol). The injection volumes were 50 μL. The refractive index detector gains toward MDI and PTMO prepolymers were determined by representing the areas under their corresponding chromatograms versus the injected masses [Figure 5(a)]. From Figure 5(a), the refractometer gains toward MDI and PTMO resulted $C_{\text{DR,MDI}} = 2.02 \times 10^{-3}$ (a.u.) and $C_{\text{DR,PTMO}} = 1.3 \times 10^{-3}$ (a.u.), respectively. The molar masses were estimated from the calibration curve of Figure 5(b). The calibration was obtained by fitting a third-order polynomial to the chromatograms of 17 standards from PPS

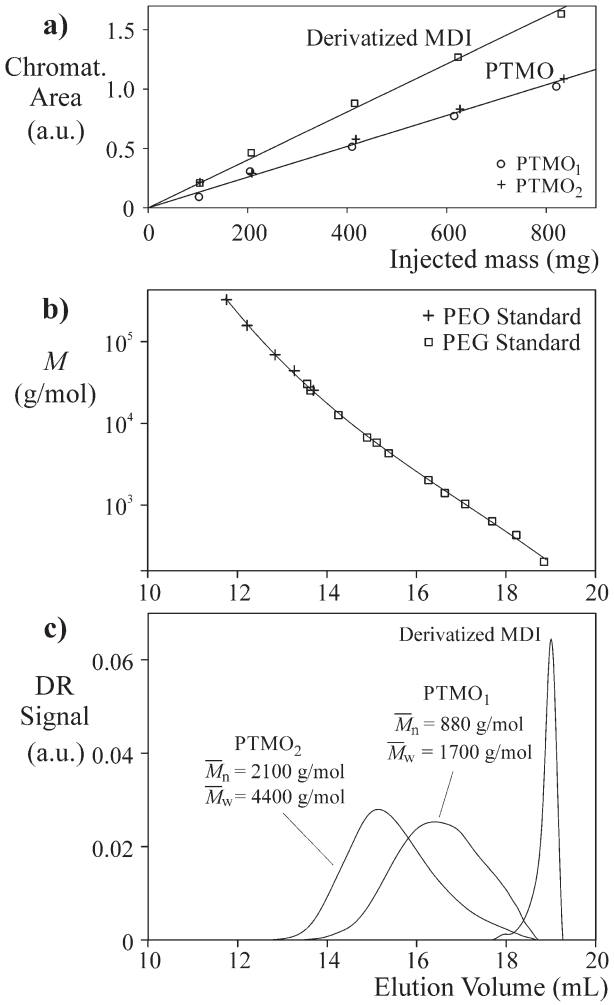

Figure 5. SEC measurements of the initial reagents. (a) Estimation of the differential refractometer (DR) gains toward MDI and PTMO. (b) Molar mass calibration obtained from PEG and PEO standards at 25 °C in THF. (c) Baseline-corrected chromatograms of the initial MDI and prepolymers. The MDI chromatogram suggests the presence of a dimer contaminant.

Polymer Standards Service GmbH; consisting of 12 lower molar mass standards of poly(ethylene glycol) (PEG), and 5 higher molar mass standards of poly(ethylene oxide) (PEO). Figure 5(c) represents the baseline-corrected chromatograms for MDI, PTMO_1, and PTMO_2. The MDI chromatogram exhibits a small peak at elution time 18 mL that suggests contamination by its dimer. Also presented in Figure 5(c) are the average molar masses of PTMO_1 and PTMO_2, as determined by SEC. In Table I, these values are compared with backtitration measurements carried out by the manufacturer and in our laboratory. Backtitration errors are caused by the relatively high dilution of end groups. SEC errors of $\bar{M}_n$ values are caused by: (a) lack of appropriate calibration standards, and (b) contamination at the low molar masses by peaks from the solvent and other low molar mass compounds. The initial macrodiol masses (upper rows of Table II) were based on the $\bar{M}_n$ estimates provided by the manufacturer; and errors in such estimates directly affect reaction stoichiometry and the final attainable molar masses.

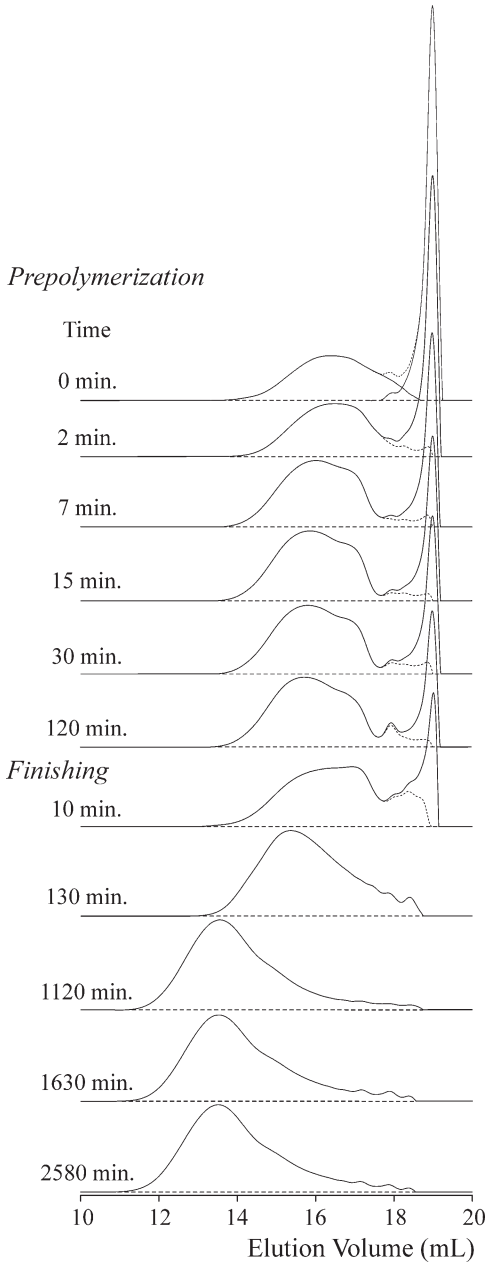

Figure 6. Experiment 1. Normalized and baseline-corrected DR chromatograms of the derivatized samples along the reaction. The total chromatogram shown at the beginning of the prepolymerization ($t_{Prep.} = 0$ min) was estimated by addition of the individual chromatograms of $PTMO_1$ and MDI according to their weight fractions and DR gains [Figure 5(a)].

For experiment 1, Figure 6 presents the normalized and baseline-corrected chromatograms at several reaction samples. At the start of the prepolymerization ($t_{Prep.} = 0$ min), the total chromatogram was estimated by addition of the MDI and $PTMO_1$ chromatograms of Figure 5(c), appropriately weighed by their mass concentrations and detector gains as determined in Figure 5(a). Along the prepolymerization, the chromatograms of the polymer alone (i.e., without the MDI in excess) were obtained by subtraction of the MDI peaks (shown in gray) from the total chromatograms (Figure 6).

The main SEC results are in shown in Figure 7, and in Tables II and III, and Supporting Information Table S3. Figure 7 presents the MMDs of the polymers alone (i.e., without the MDI or BD) at the end of each reaction stage. Table III and Supporting Information Table S3 present: (a) the average molar masses of the polymers alone ($\bar{M}_{n,Pol.}$ and $\bar{M}_{w,Pol.}$) along the complete reaction; and (b) the following variables along the prepolymerization: the mass fraction of unreacted MDI ($\omega_{MDI,Prep.}$), and the global $\bar{M}_n$ values ($\bar{M}_{n,Global\ Prep.}$). (Note that $\omega_{MDI,Fin.}$ and $\bar{M}_{n,Global\ Fin.}$ cannot be estimated along the finishing stage because the SEC samples did not contain the unreacted BD.) Along the prepolymerization, $\omega_{MDI,Prep.}$ and $\bar{M}_{n,Global\ Prep.}$ were estimated through

$$\omega_{MDI,Prep.} = \frac{C_{DR,MDI}\ (\text{Area under MDI peak})}{C_{DR,MDI}\ (\text{Area under MDI peak}) + C_{DR,PTMO}\ (\text{Area under polymer peak})} \quad (10)$$

$$\frac{1}{\bar{M}_{n,Global\ Prep.}} = \frac{\omega_{MDI,Prep.}}{M_{MDI}} + \frac{\left(1-\omega_{MDI,Prep.}\right)}{\bar{M}_{n,Pol.}} \quad (11)$$

where $C_{DR,MDI}$ and $C_{DR,PTMO}$ are refractometer gains; and $M_{MDI} = 250.25$ g mol^{-1} is the molar mass of MDI.

Consider the average molar masses at the prepolymerization ends (Tables II and III, and Supporting Information Table S3). In experiment 1, the global number-average molar mass ($\bar{M}_{n,Global}$) was estimated by ^{1}H-NMR and by SEC, and the ^{1}H-NMR technique provided a higher value than SEC. Possible reasons for this difference are: (a) underestimation of —NCO end groups by ^{1}H-NMR, due to an incomplete derivatization; and (b) presence of negative peaks at the high retention volumes of the SEC chromatograms, that reduce the MDI peak area. The

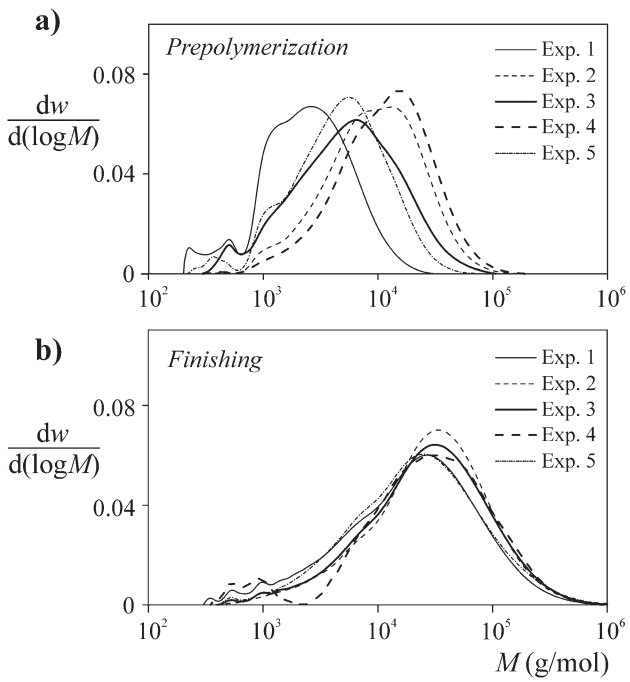

Figure 7. MMDs of experiments 1–5 at the prepolymerization end (a) and at the reaction end (b).

Table IV. Kinetic Constants Adjusted in this Work at $T = 60\,^{\circ}C$ and Reported Literature Constants Obtained in Similar Reactions

		This work	Literature values
Prepolymerization	k_1 (L mol^{-1} s^{-1})	1.07×10^{-3}	2.67×10^{-4}[a] and 6.17×10^{-5}[b] (Sun and Sung[20])
Finishing	k_2 (L mol^{-1} s^{-1})	1.94×10^{-4}	6.55×10^{-5} (Majoros *et al.*[22])

[a] For conversions < 50%.
[b] For conversions > 50%.

following conditions are expected to increase the polymer average molar masses ($\bar{M}_{n,\mathrm{Pol.}}$ and $\bar{M}_{w,\mathrm{Pol.}}$): (a) the use of $PTMO_2$ rather than $PTMO_1$, since $\bar{M}_{n,\mathrm{PTMO_2}} > \bar{M}_{n,\mathrm{PTMO_1}}$; and (b) a lower excess of MDI. Experiments 1 and 3 involve identical recipes and reaction conditions except for the employed macrodiol; and similarly with experiments 2 and 4. This explains the higher molar masses of experiment 3 with respect to experiment 1, and of experiment 4 with respect to experiment 2. Also, experiment 2 employs a lower excess of MDI than experiment 1; and similarly experiment 3 employs a lower excess of MDI than experiment 4. This explains the higher molar masses of experiment 2 with respect to experiment 1, and of experiment 4 with respect to experiment 3 (Tables II and III, and Supporting Information Table S3). Finally, note that the lower excess of MDI in experiments 2 and 4 also involved longer reaction times to attain steady-state values than experiments 1 and 3.

Estimation of Rate Constants

"Effective" rate constants for the prepolymerization and finishing stages were estimated on the basis of the ^{1}H-NMR measurements for experiment 1. For each reaction stage and independently of stoichiometry, the following mass balances can be written

$$\frac{dn_{-\mathrm{NCO,theor.}}}{dt}(t) = -\,k_i'\left[n_{-\mathrm{NCO,theor.}}(t) \times n_{-\mathrm{OH,theor.}}(t)\right] \quad \text{with } n^0_{-\mathrm{NCO,Prep.}} \text{ and } n^0_{-\mathrm{NCO,Fin.}} \tag{12a}$$

$$\frac{dn_{-\mathrm{OH,theor.}}}{dt}(t) = -\,k_i'\left[n_{-\mathrm{NCO,theor.}}(t) \times n_{-\mathrm{OH,theor.}}(t)\right] \quad \text{with } n^0_{-\mathrm{OH,Prep.}} \text{ and } n^0_{-\mathrm{OH,Fin.}} \tag{12b}$$

$$\frac{dn_{-\mathrm{NHCOO-,theor.}}}{dt}(t) = k_i'\left[n_{-\mathrm{NCO,theor.}}(t) \times n_{-\mathrm{OH,theor.}}(t)\right] \quad \text{with } n^0_{-\mathrm{NHCOO-,Prep.}} \text{ and } n^0_{-\mathrm{NHCOO-,Fin.}} \tag{12c}$$

$$k_i' = \frac{k_i}{V_i} \qquad \text{with } n^0_{\mathrm{Prep.}} \text{ or } n^0_{\mathrm{Fin.}} \tag{12d}$$

where $n_{-\mathrm{NCO,theor.}}(t)$, $n_{-\mathrm{OH,theor.}}(t)$, and $n_{-\mathrm{NHCOO-,theor.}}(t)$ are the model predictions; V_i is the reaction volume, with $V_{\mathrm{Prep.}} = 3.49$ mL or $V_{\mathrm{Fin.}} = 23.1$ mL; k_i' is a molar-based rate constant (in mol^{-1} s^{-1}) that represents either k_1' or k_2'; and k_i is a concentration-based rate constant (in L mol^{-1} s^{-1}) that represents either the prepolymerization rate constant (k_1), or the finishing rate constant (k_2). The kinetic constants were estimated by comparing the model predictions $n_{-\mathrm{NCO,theor.}}(t)$ and $n_{-\mathrm{NHCOO-,theor.}}(t)$ with their corresponding measurements (Figure 3). More specifically, k_1' and k_2' were independently adjusted through the following minimization algorithm:

$$\min_{(k_i')} \; E = w_1 \frac{1}{N}\sum_1^N \left| \frac{n_{-\mathrm{NCO,peak\ a}} - n_{-\mathrm{NCO,theor.}}}{n_{-\mathrm{NCO,peak\ a}}} \right| + w_2 \frac{1}{N}\sum_1^N \left| \frac{n_{-\mathrm{NCO,peak\ b}} - n_{-\mathrm{NCO,theor.}}}{n_{-\mathrm{NCO,peak\ b}}} \right| + w_3 \frac{1}{N}\sum_1^N \left| \frac{n_{-\mathrm{NHCOO-,peak\ f}} - n_{-\mathrm{NHCOO-,theor.}}}{n_{-\mathrm{NHCOO-,peak\ f}}} \right|$$
$$\text{with } (w_1 = w_2 = 0.5;\ \ w_3 = 1);\ \ (N = 5) \tag{13}$$

where E is an error functional; $n_{-\mathrm{NCO,peak\ a}}$ and $n_{-\mathrm{NCO,peak\ b}}$ are the moles of isocyanate groups estimated by ^{1}H-NMR through peaks a and b, respectively; $n_{-\mathrm{NHCOO-,peak\ f}}$ are the moles of urethane groups estimated through peak f; N (=5) is the number of measurements employed in each reaction stage; and w_i's are the adopted weighting factors.

Equations (12a)–(12c) were integrated through an explicit Runge–Kutta algorithm. The following initial conditions were employed: (a) for the prepolymerization, two different sets of initial conditions were used: one based on the nominal recipe of experiment 1, i.e., $n^0_{-\mathrm{NCO,Prep.}} = 1.34 \times 10^{-2}$ mol, $n^0_{-\mathrm{OH,Prep.}} = 4.02 \times 10^{-3}$ mol, and $n^0_{-\mathrm{NHCOO-,Prep.}} = 0$ mol [see points (A,A′) in Figure 3]; and another based on the ^{1}H-NMR estimates by peak a [see values in Table III and points (B,B′) in Figure 3]; and (b) for the finishing stage, only the initial conditions based on the ^{1}H-NMR estimates by peak a were employed (Table III).

The resulting rate constants are presented on the left hand side of Table IV, and the model predictions obtained from such constants are shown in continuous trace in Figure 3(a,b). Two slightly different estimates were obtained for k_1, according to the employed initial conditions, and their average is presented in Table IV. As expected from the retarding effect of THF along the finishing stage,[21] the prepolymerization rate constant ($k_1 = 1.07 \times 10^{-3}$ L mol^{-1} s^{-1}) is higher than the finishing rate constant ($k_2 = 1.94 \times 10^{-4}$ L mol^{-1} s^{-1}). Table IV compares the new rate constants with reported literature values. The prepolymerization rate constant is compared to the values reported by Sun and Sung[20] for a similar bulk polymerization carried out at 60 °C between MDI and PPG (rather than PTMO). The reaction assumed second-order kinetics, and two values were reported according to conversion.[20] Other differences with the present work are that the reactions by Sun and Sung[20] were non-stirred and in stoichiometric equilibrium (rather than with diisocyanate in excess). The finishing rate constant is compared to the value reported by Majoros *et al.*[22] for a similar solution polymerization. The reactions by Majoros

et al.[22] were also carried out at 60 °C and with THF as solvent, but differed in the employed reagents: PPG was used instead of PTMO, and 2,4- and 2,6-TDI were used instead of MDI.[22] Another difference is that the reactions by Majoros *et al.*[22] were carried out with an excess of TDI, rather than in stoichiometric equilibrium.[22]

Verification of Two Classical Probabilistic Expressions

For linear polymers obtained from comonomers AA and BB, Flory theoretically predicted the evolution (with extent of reaction) of the chain length distribution and average chain lengths.[33,34] The models were based on the following assumptions: (a) the reaction rate is independent of chain length; and (b) intramolecular and secondary reactions are neglected. In our case, a molar mass-distributed macrodiol was employed rather than a low molar mass diol; and two different types of repeating units are produced along the finishing stage. The prepolymerization was carried out in excess of MDI, and the finishing stage was carried out under stoichiometric equilibrium. Therefore, the following expressions are applicable for the evolution (with extent of reaction) of the global number-average number of structural units generated along prepolymerization and finishing stages[33,34]

$$\bar{x}_{n,\mathrm{Prep.}}\left(p_{\mathrm{Prep.}}\right)=\frac{1+r}{1+r-2\ r\ p_{\mathrm{Prep.}}} \tag{14a}$$

$$\bar{z}_{n,\mathrm{Fin.}}\left(p_{\mathrm{Fin.}}\right)=\frac{1}{1-p_{\mathrm{Fin.}}} \tag{14b}$$

where r is the ratio between the initial number of end groups in defect and the initial number of end groups in excess.

For experiment 1, $r = 0.3$ (Table II), and eq. (14) is represented in continuous trace in Figure 4. Along the prepolymerization, an excellent agreement is observed; while larger errors are observed along the finishing stage (Figure 4). This seems reasonable, bearing in mind that the experimental estimates were based on the analysis of end groups, and their concentrations fall drastically when the extent of reaction approaches unity. In addition, the estimate of $\bar{z}_{n,\mathrm{Fin.}}$ is more subject to error than $\bar{x}_{n,\mathrm{Prep.}}$, because it is based on a difference between urethane moles [compare eq. (9)]. Note, finally that $\bar{x}_{n,\mathrm{Prep.}}$ or $\bar{z}_{n,\mathrm{Fin.}}$ cannot be used to estimate the corresponding global number-average molar masses. This is because $\bar{x}_{n,\mathrm{Prep.}}$ includes the MMD of the initial PTMO, and $\bar{z}_{n,\mathrm{Fin.}}$ does not contain information on the concentration of the two different types of structural units (the soft and hard segments). Note that these results cannot be interpreted in terms of kinetic constants, since the independent variable is extent of reaction rather than reaction time.

CONCLUSIONS

This study highlights the difficulties in quantifying the synthesis of linear PUs. The difficulties arise from uncertainties in the quality of the reagents, in the reaction recipes, in the adopted reaction mechanism, and in the measurements. In turn, all of these errors affect the estimated rate constants. With regard to quality of reagents: (1) not all macrodiol molecules are necessarily linear and/or contain hydroxyl reactive groups at their chain ends; and (2) the MDI consists of a mixture of different isomers and dimers. With regard to recipe problems, the macrodiol masses were estimated from the $\bar{M}_n$ values provided by their manufacturer, while different values were estimated in this work (Table I). With regard to polymerization mechanism, intramolecular, secondary, and autocatalytic reactions were neglected. In reality however: (a) intramolecular reactions are known to lower the $\bar{M}_n$ value of the final polymer, and to increase molar mass dispersity[34]; (b) secondary reactions may reduce the total concentration of isocyanate groups; and (c) autocatalytic reactions may increase the global reaction rate. With regard to measurement errors, the following was observed: (1) by SEC, large errors are introduced into the $\bar{M}_n$ estimates, due to presence of low molar mass contaminants and/or unreacted comonomers; and (2) by ^{1}H-NMR, biases in the determination of (terminal and internal group) concentrations directly affect the rate constants and the estimates of extent of reaction and number-average number of structural units. Unfortunately, the unreacted hydroxyl groups could not be measured, and were indirectly estimated through eqs. (5) and (6). At high conversions of the finishing stage, large errors are expected due to: (a) the high dilution of isocyanate end groups; and (b) the absence of truly stoichiometric conditions, as required by eq. (6). Finally, note that the number-average number of structural units ($\bar{z}_{n,\mathrm{Fin.}}$) was estimated from a difference between the total number of urethane groups and the urethane groups at the end of the prepolymerization [eq. (9b)]. These last errors explain the relatively large differences observed in Figure 4 at high conversions of the finishing stage with respect to the theoretical predictions of eq. (14).

The rate constants estimated in this work (Table IV) were calculated from the ^{1}H-NMR measurements of experiment 1, and are therefore affected by many of the previously mentioned sources of error. Such estimates were also seen to be affected by errors in the initial concentrations of reactive groups, where a difference of about 17% is observed between the nominal recipe values and the ^{1}H-NMR measurements (Table II). All the aforementioned reasons explain the difficulties in quantifying the effect of the different sources of error into the estimated rate constants, and also explains the relatively large differences between the new estimates and literature values for similar reaction systems (Table IV).

With simple kinetic models such as eq. (12), the information on MMDs and averages obtained by SEC cannot be used to adjust the rate constants presented here. In the second part of this sequel, a new comprehensive polymerization model is presented that predicts the time evolution of the MMD and averages along the analyzed reactions; and that model enables a final readjustment of the here presented rate constants.

ACKNOWLEDGMENTS

The authors wish to express their gratitude to CONICET (grant no. PIP2011 848), MINCyT (grant no. PICT2011 1254), Universidad Nacional del Litoral (grant no. CAI + D2011 419), and MINCyT-COLCIENCIAS (grant no. CO/11/02) for the project funding.

REFERENCES

1. Król, P. Linear Polyurethanes: Synthesis Methods, Chemical Structures, Properties and Applications; VSP: Leiden, **2008**.
2. Eceiza, A.; de la Caba, K.; Kortaberria, G.; Gabilondo, N.; Marieta, C.; Corcuera, M. A.; Mondragon, I. *Eur. Polym. J.* **2005**, *41*, 3051.
3. Yilgor, I.; Yilgor, E.; Guler, I. G.; Ward, T. C.; Wilkes, G. L. *Polymer* **2006**, *47*, 4105.
4. Lee, D.; Speckhard, T. A.; Sorensen, A. D.; Cooper, S. L. *Macromolecules* **1986**, *19*, 2383.
5. Yilgör, I.; Yilgör, E.; Wilkes, G. L. *Polymer* **2015**, *58*, A1.
6. Eceiza, A.; Zabala, J.; Egiburu, J. L.; Corcuera, M. A.; Mondragon, I.; Pascault, J. P. *Eur. Polym. J.* **1999**, *35*, 1949.
7. Yilgor, I.; Yilgor, E. *Polym. Rev.* **2007**, *47*, 487.
8. Hood, M. A.; Wang, B.; Sands, J. M.; La Scala, J. J.; Beyer, F. L.; Li, C. Y. *Polymer* **2010**, *51*, 2191.
9. Castagna, A. M.; Fragiadakis, D.; Lee, H.; Choi, T.; Runt, J. *Macromolecules* **2011**, *44*, 7831.
10. Spaans, C. J.; Groot, J. H.; De, Dekens, F. G.; Pennings, A. J. *Polym. Bull.* **1998**, *41*, 131.
11. Spaans, C. J.; De Groot, J. H.; Belgraver, V. W.; Pennings, A. J. *J. Mater. Sci. Mater. Med.* **1998**, *9*, 675.
12. Król, P.; Pilch-Pitera, B. *Eur. Polym. J.* **2003**, *39*, 1229.
13. Castro, J. M.; Lopez-Serrano, F.; Camargo, R. E.; Macosko, C. W.; Tirrell, M. *J. Appl. Polym. Sci.* **1981**, *26*, 2067.
14. Chen, C. H. Y.; Briber, R. M.; Thomas, E. L.; Xu, M.; MacKnight, W. J. *Polymer* **1983**, *24*, 1333.
15. Speckhard, T. A.; Miller, J. A.; Cooper, S. L. *Macromolecules* **1986**, *19*, 1558.
16. Caraculacu, A. A.; Coseri, S. *Prog. Polym. Sci.* **2001**, *26*, 799.
17. Grepinet, B.; Pla, F.; Hobbes, P. H.; Swaels, P. H.; Monge, T. H. *J. Appl. Polym. Sci.* **2000**, *75*, 705.
18. Grepinet, B.; Pla, F.; Hobbes, P.; Monge, T.; Swaels, P. *J. Appl. Polym. Sci.* **2001**, *81*, 3149.
19. Hailu, K.; Guthausen, G.; Becker, W.; König, A.; Bendfeld, A.; Geissler, E. *Polym. Test.* **2010**, *29*, 513.
20. Sun, X.-D.; Sung, C. S. P. *Macromolecules* **1996**, *29*, 3198.
21. Chang, M.-C.; Chen, S.-A. *J. Polym. Sci. Part A: Polym. Chem.* **1987**, *25*, 2543.
22. Majoros, L. I.; Dekeyser, B.; Hoogenboom, R.; Fijten, M. W. M.; Geeraert, J.; Haucourt, N.; Schubert, U. S. *J. Polym. Sci. Part A: Polym. Chem.* **2010**, *48*, 570.
23. Kothandaraman, H.; Nasar, A. S. *J. Macromol. Sci. Part A: Pure Appl. Chem.* **1994**, *31*, 339.
24. Chokki, Y.; Nakabayashi, M.; Sumi, M. *Die Makromol. Chem.* **1972**, *153*, 189.
25. Chokki, Y. *Die Makromol. Chem.* **1974**, *175*, 3424.
26. Yeager, F. W.; Becker, J. W. *Anal. Chem.* **1977**, *49*, 722.
27. Dubois, C.; Désilets, S.; Ait-Kadi, A.; Tanguy, P. *J. Appl. Polym. Sci.* **1995**, *58*, 827.
28. Thompson, C. M.; Taylor, S. G.; McGee, W. W. *J. Polym. Sci. Part A: Polym. Chem.* **1990**, *28*, 334.
29. Aust, N.; Gobec, G. *Macromol. Mater. Eng.* **2001**, *286*, 119.
30. Król, P.; Wojturska, J. *J. Appl. Polym. Sci.* **2003**, *88*, 327.
31. Król, P. *J. Appl. Polym. Sci.* **1995**, *57*, 739.
32. Sato, M. *J. Am. Chem. Soc.* **1960**, *82*, 3893.
33. Flory, P. J. *J. Am. Chem. Soc.* **1936**, *58*, 1877.
34. Flory, P. J. Principles of Polymer Chemistry; Cornell University Press: New York, **1953**.